

Electronic Supplementary Information

Porous NanoMoC@Graphite Shell Derived from MOFs-Directed Strategy: Efficient Electrocatalyst for Hydrogen Evolution Reaction

Zhangping Shi,^a Yangxia Wang,^a Huanlei Lin,^b Hongbin Zhang,^a Meikun Shen,^a
Songhai Xie,^a Yahong Zhang,^a Qingsheng Gao^{*b} and Yi Tang^{*a}

^a Department of Chemistry, Shanghai Key Laboratory of Molecular Catalysis and Innovative Materials, Laboratory of Advanced Materials and Collaborative Innovation Center of Chemistry for Energy Materials, Fudan University, No. 220 Handan Road, 200433 Shanghai, P. R. China. E-mail: yitang@fudan.edu.cn

^b Department of Chemistry, Jinan University, No. 601 Huangpu Avenue West, 510632 Guangzhou, P. R. China. E-mail: tqsgao@jnu.edu.cn

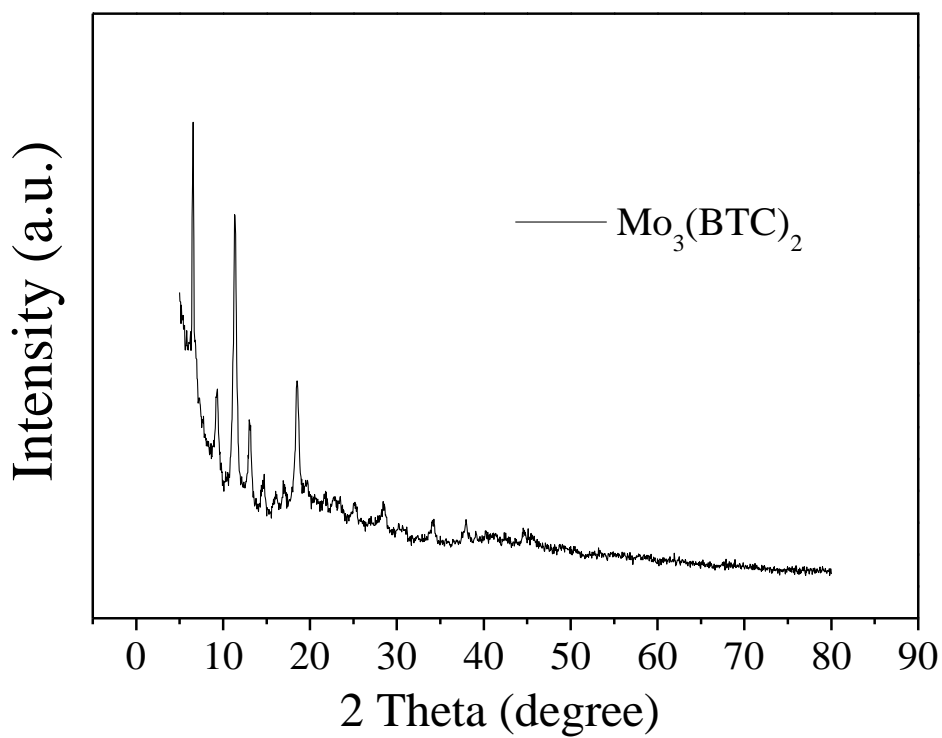


Fig. S1. XRD pattern of $\text{Mo}_3(\text{BTC})_2$ precursor

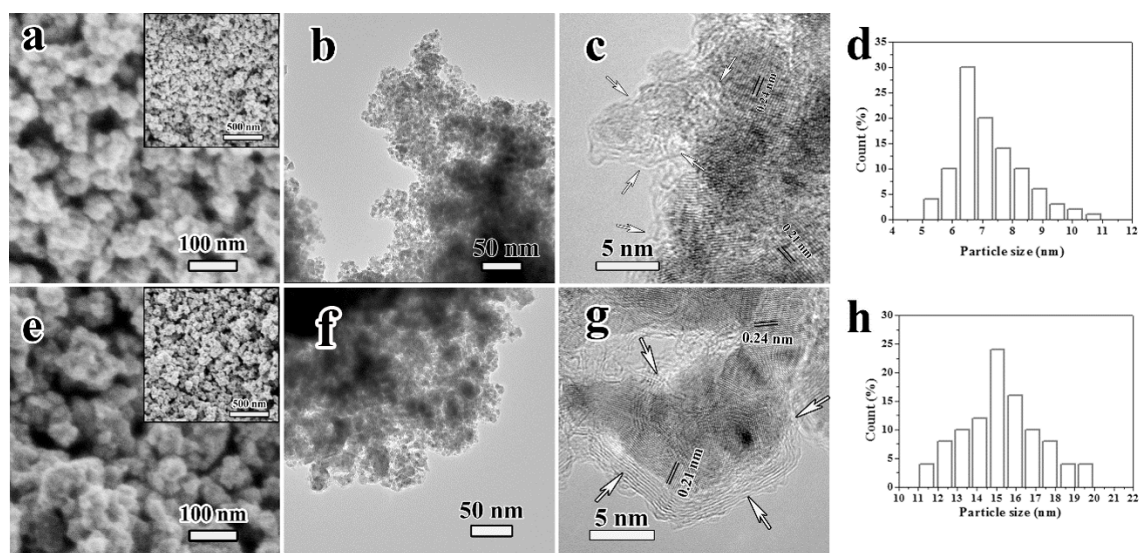


Fig. S2. SEM (a) and TEM images (b, c) of nanoMoC@GS(800); SEM (e) and TEM images (f, g) of nanoMoC@GS(900); (d, h) Particle size distribution of the MoC nanoparticles of nanoMoC@GS(800) and nanoMoC@GS(900), respectively.

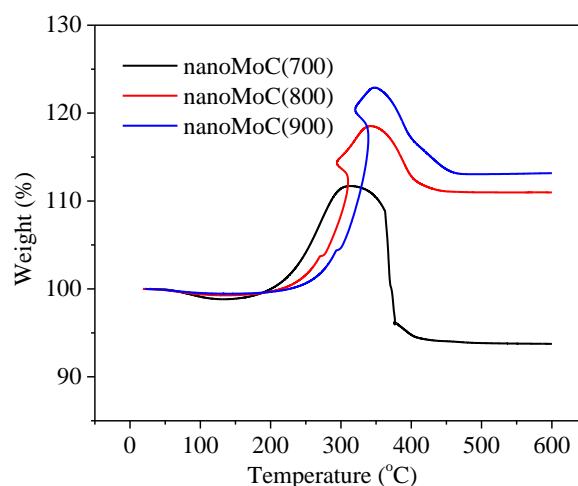


Fig. S3. TGA curve of nanoMoC@GS samples for measurement of the carbon content. The initial weight gained below 350 °C was due to the gradual oxidation of MoC_x to MoO₃, followed by a significant weight loss caused by the combustion of carbon. Assuming that the sample was composed of stoichiometric MoC and carbon, and converted to only MoO₃ after heating to 600 °C with remaining weight of *c* wt.%, the carbon content in the shell (free carbon not including the carbon in MoC species) is estimated according to the following the equation of $m(\text{carbon}) = 1 - c \text{ wt.}\% \cdot M(\text{MoC})/M(\text{MoO}_3) = y \text{ wt.}\%$. Additionally, the Mo content of those catalysts are also quantified by ICP-AES to confirm the TGA results.^{S1}

Table S1. The contents of each component in nanoMoC@GS samples.

Sample	Carbon in shell (wt.%) ^a	MoC (wt.%) ^a	MoC (wt.%) ^b
nanoMoC@GS(700)	30	70	68
nanoMoC@GS(800)	19	81	78
nanoMoC@GS(900)	15	85	86

^a calculated according to the TGA curves.

^b quantified by ICP-AES. 5 mg nanoMoC@GS was dispersed in hydrogen peroxide solution (30 %), and decomposed by stirring. After filtration, the solution was diluted to 50 ml in a volumetric flask for the ICP-AES test. It was found that the contents of MoC determined by TGA and ICP-AES almost gave the same results, confirming the feasibility of the two methods for the detailed element analysis.

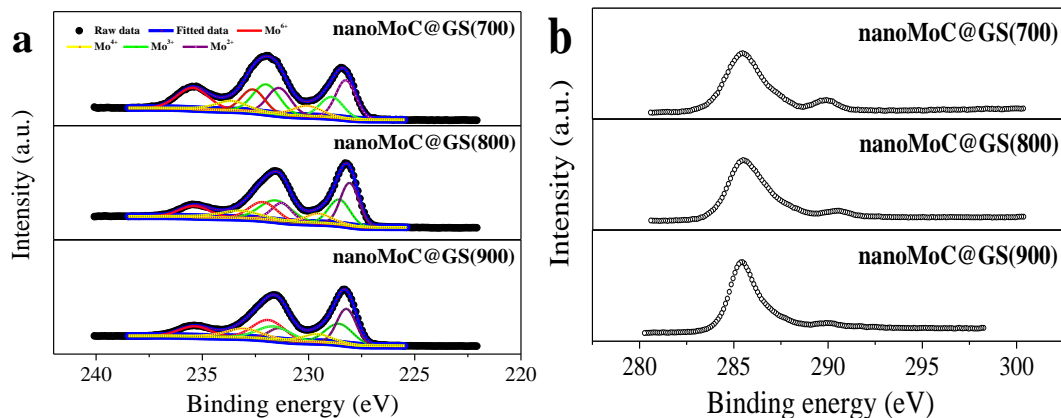


Fig. S4. (a) Mo 3d XPS profiles of the as-obtained nanoMoC@GS materials; (b) C 1s XPS profiles of the as-obtained nanoMoC@GS materials.

Table S2. Fitting parameters (peak position, peak area and species percentage) for both Mo 3d_{5/2} and Mo 3d_{3/2} spectra taken on nanoMoC@GS.

Sample	species	B. E. (eV)		Area		Mo ³⁺ /Mo ²⁺	Mo ³⁺ and Mo ²⁺ (%)
		3d _{5/2}	3d _{3/2}	3d _{5/2}	3d _{3/2}		
nanoMoC@GS(700)	Mo ²⁺	228.3	231.4	25194	19430	0.9	61.3
	Mo ³⁺	228.9	232.0	15841	24465		
	Mo ⁴⁺	230.0	233.4	8911	5876		
	Mo ⁶⁺	232.4	235.5	18307	20603		
nanoMoC@GS(800)	Mo ²⁺	228.2	231.3	65227	27266	1.1	62.7
	Mo ³⁺	228.8	231.8	52734	44856		
	Mo ⁴⁺	229.8	233.3	19831	24039		
	Mo ⁶⁺	232.3	235.4	41649	27384		
nanoMoC@GS(900)	Mo ²⁺	228.3	231.4	93440	33283	1.3	56.0
	Mo ³⁺	228.7	231.7	73581	53833		
	Mo ⁴⁺	229.8	233.3	30876	40858		
	Mo ⁶⁺	232.5	235.4	85807	42493		

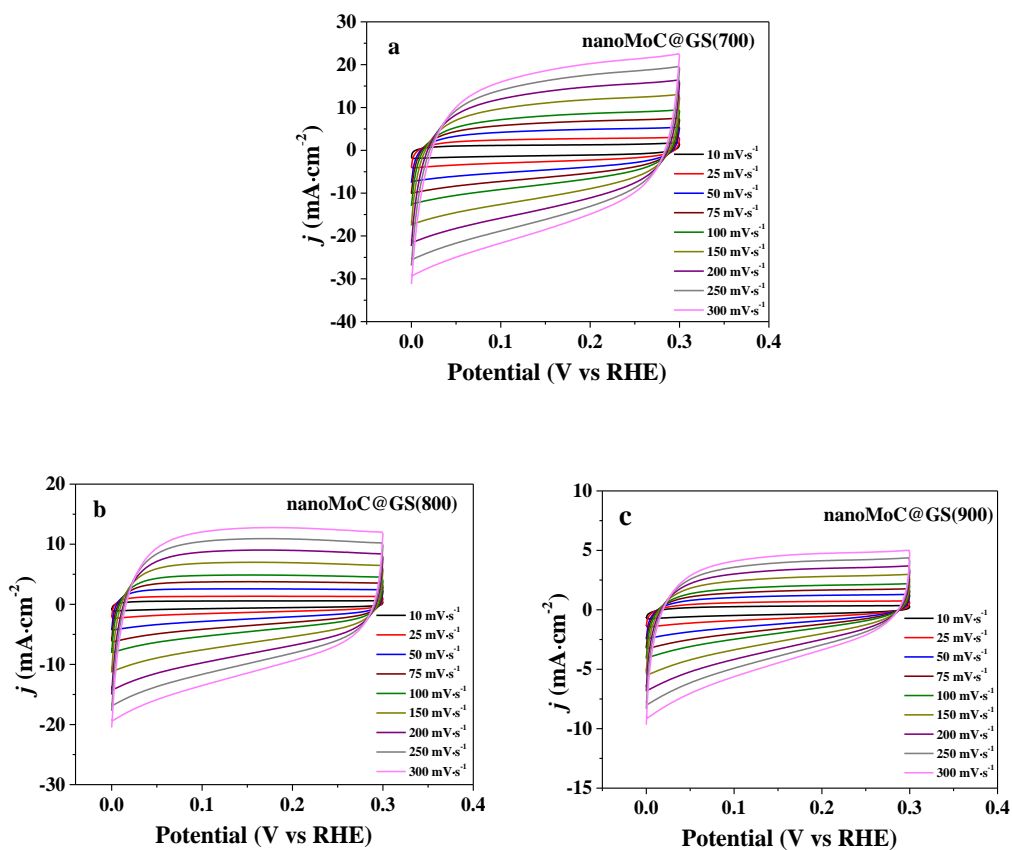


Fig. S5. Cyclic voltammograms (CVs) for nanoMoC@GS(700) (a), nanoMoC@GS(800) (b) and nanoMoC@GS(900) (c) with different rates from 10 to 300 mV·s⁻¹ in the potential range of 0-0.3 V in 0.5 M H₂SO₄. C_{dl} can be used to represent the electrochemical surface area (ESCA) of nanoMoC@GS. NanoMoC@GS(700) has the largest active surface area and thus possesses the most amount of active sites and exposed edges for HER.

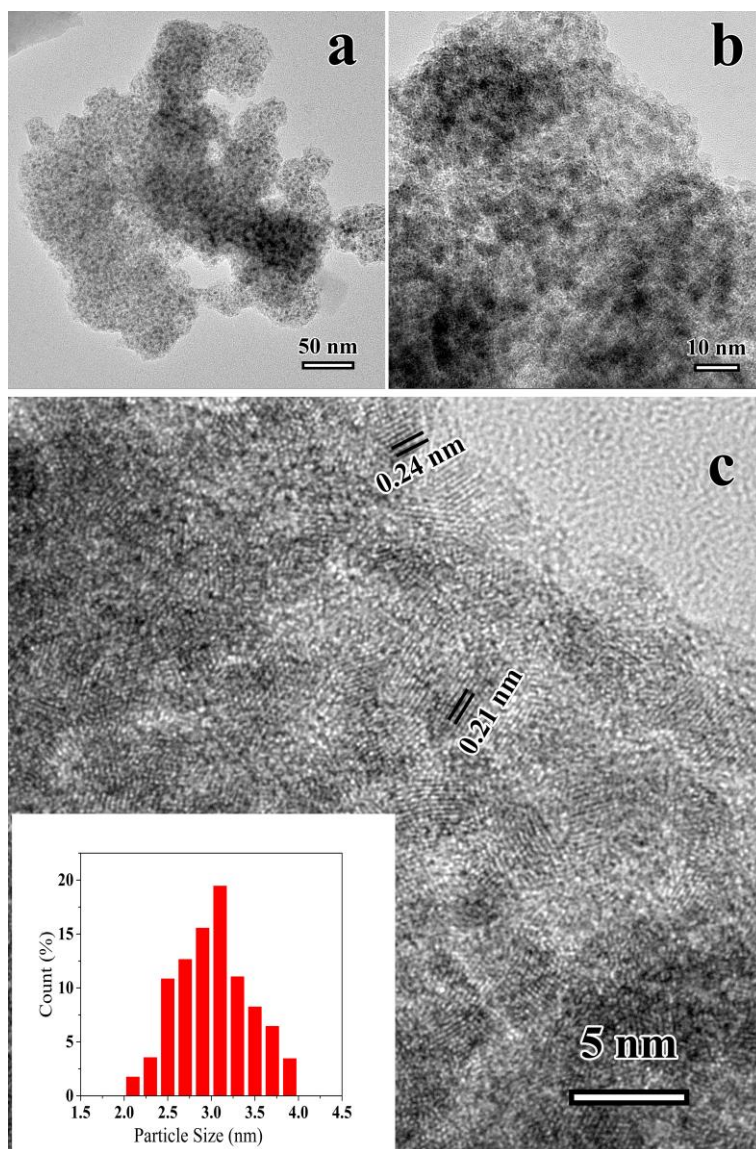


Fig. S6. TEM images (a, b and c) of nanoMoC@GS(700) after electrochemical stability test. Inset of c is the particle size distribution of the MoC nanoparticles of nanoMoC@GS(700) after electrochemical stability test.

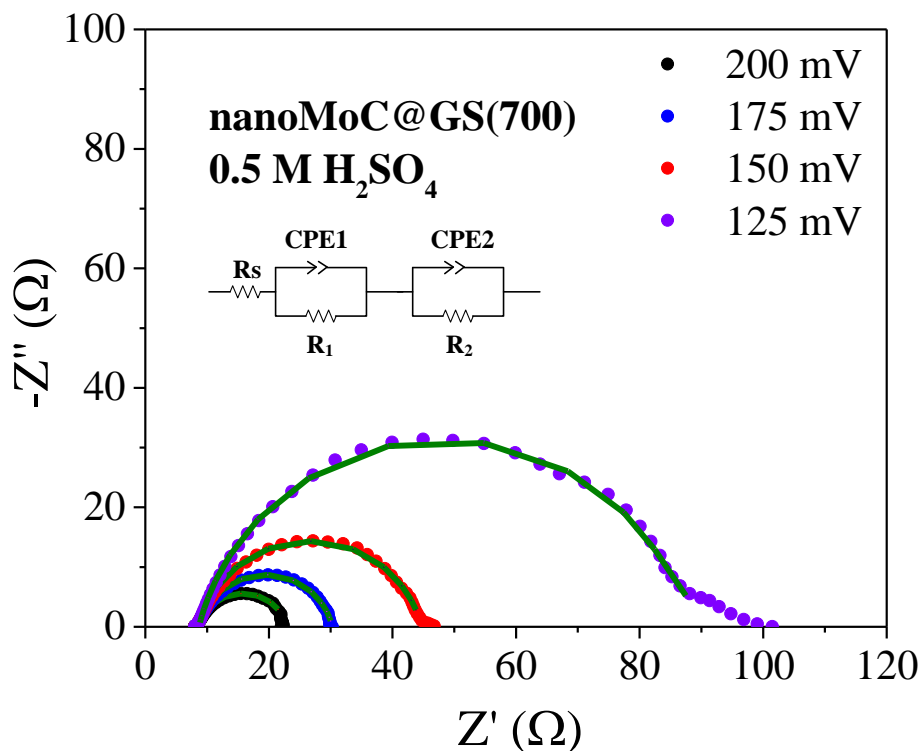


Fig. S7. Electrochemical impedance spectroscopy (EIS) for nanoMoC@GS(700) under different overpotential in 0.5 M H_2SO_4 , the data are fitted to the simplified equivalent circuit shown in the inset, and the fitting results are plotted as solid traces. Inset is the Equivalent circuit model for electrochemical impedance tests. R_s , R_1 and R_2 represent the electrolyte, electrode porosity and charge transfer resistance, respectively. CPE is the constant phase angle element, which represents the double layer capacitance of solid electrode in the real-world situation. So, R_1 suggested that this electrocatalyst processed an abundant porosity of the obtained nanoMoC@GS catalysts. R_2 was related to electrode kinetics of the obtained materials, and nanoMoC@GS(700) with the small value at the same overpotentials suggested a rapid charge transfer kinetics during the electrochemical process.

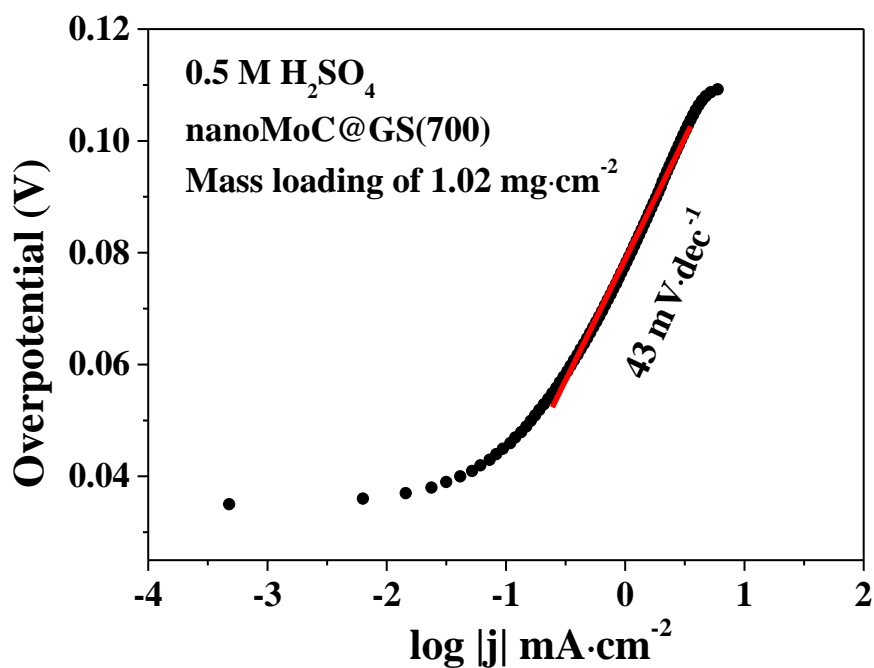


Fig. S8. The Tafel plots of nanoMoC@GS(700) with a mass loading of $1.02 \text{ mg}\cdot\text{cm}^{-2}$ in $0.5 \text{ M H}_2\text{SO}_4$.

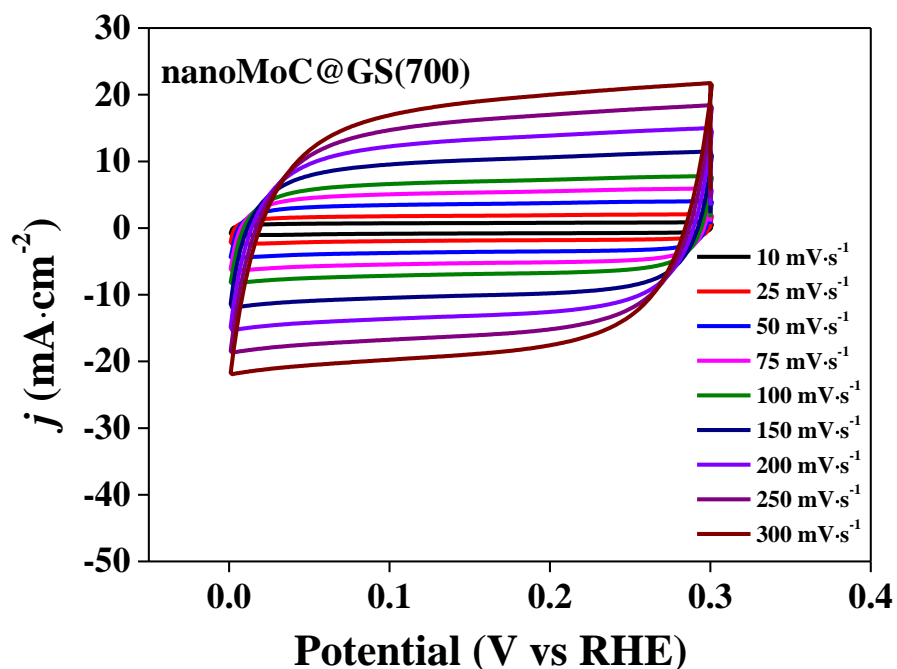


Fig. S9. Cyclic voltammograms (CVs) for nanoMoC@GS(700) with different rates from 10 to 300 $\text{mV}\cdot\text{s}^{-1}$ in the potential range of 0-0.3 V in 1.0 M KOH .

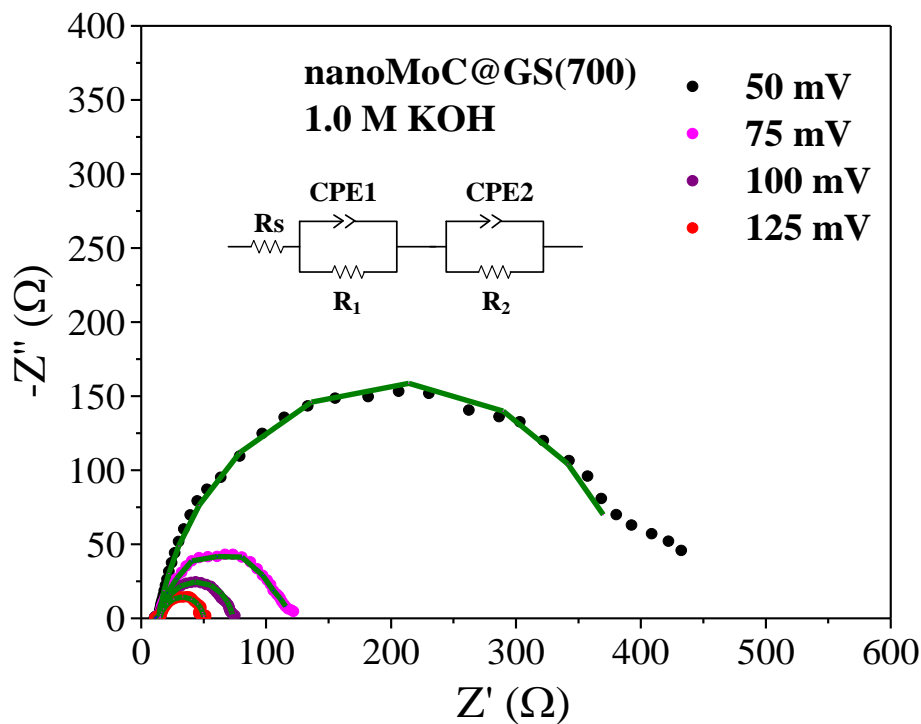


Fig. S10. Electrochemical impedance spectroscopy (EIS) for nanoMoC@GS(700) under different overpotential in 1.0 M KOH, the data are fitted to the simplified equivalent circuit shown in the inset, and the fitting results are plotted as solid traces.

Table S3. Summary of HER activities of nanoMoC@GS materials.

Electrolyte	Sample	η_1 (mV)	η_{10} (mV)	j ($\eta=200$) (mA·cm ⁻²)	Tafei slope (mV·dec ⁻¹)	j_0^c (mA·cm ⁻²)
Acidic media.	nanoMoC@GS(700) ^a	84	132	100	46	13.5×10^{-3}
	nanoMoC@GS(700) ^b	75	124	146	43	15.1×10^{-3}
	nanoMoC@GS(800) ^a	116	159	45	51	7.0×10^{-3}
	nanoMoC@GS(900) ^a	129	185	18	56	5.5×10^{-3}
Basic media	nanoMoC@GS(700) ^a	43	77	-	50	0.212

^a: HER activity data are collected with the mass loading of 0.76 mg·cm⁻²; ^b: HER activity data are collected with the optimal mass loading of 1.02 mg·cm⁻²; ^c: j_0 is related to the exchange current density;

Table S4. Comparison of HER performance in acid media for nanoMoC@GS with other electrocatalysts.

Catalyst	Loading (mg·cm ⁻²)	<i>j</i> (mA·cm ⁻²)	<i>η</i> (mV)	Tafel slope (mV·dec ⁻¹)	Ref.
nanoMoC@GS	0.76	1	83	46	This work
		10	132		
	1.02 (optimal)	1	75	43	
MoC _x octahedrons	0.8 (optimal)	1	87	53	<i>Nat. Commun.</i> 2015 , 6, 6512.
		10	142		
MoC-RGO	0.8	10	150	57	<i>Chem. Commun.</i> , 2015 , 51, 8323.
Mo ₂ C-RGO	(optimal)	10	221	88	
Mo ₂ C NTs	0.75 (optimal)	10	172	62	<i>Angew. Chem. Int. Ed.</i> 2015 , 54, 15395.
MoC-Mo ₂ C HNWs	0.14 (optimal)	10	126	43	<i>Chem. Sci.</i> , 2016 , DOI: 10.1039/c6sc00077k.
Mo ₂ C@NC	~0.28	10	124	60	<i>Angew. Chem. Int. Ed.</i> 2015 , 54, 10752.
Mo ₂ C/CNT	2.0	10	152	65	<i>Energy Environ. Sci.</i> 2013 , 6, 943.
np-Mo ₂ C NWs	0.21	10	130	53	<i>Energy Environ. Sci.</i> 2014 , 7, 387.
MoCN	0.4	10	140	46	<i>J. Am. Chem. Soc.</i> 2015 , 137, 110.
Mo ₂ C/CNT-GR	0.65-0.67	10	130	58	<i>ACS Nano</i> 2014 , 8, 5164.
Mo ₂ C/RGO	0.285	10	130	57.3	<i>Chem. Commun.</i> 2014 , 50, 13135.
MCNs@carbon	0.25	10	78	41	<i>Angew. Chem. Int. Ed.</i> 2015 , 54, 14723.
W-Mo ₂ C NWs	1.28	10	~135	52	<i>Adv. Funct. Mater.</i> 2015 , 25, 1520.
Mo ₂ C/GCSs	0.36	10	200	62.6	<i>ACS Catal.</i> 2014 , 4, 2658.
Mo ₂ C-Mo ₂ N	1.4	10	177	-	<i>Energy Environ. Sci.</i> , 2013 , 6, 1818.
Mo ₂ C-Mo ₂ N-RGO	0.47	10	109		
MoO ₂ @PC-RGO	0.14	10	64	41	<i>Angew. Chem. Int. Ed.</i> 2015 , 54, 12928.
WO ₂ NWs	~0.35 mg	10	58	46	<i>J. Am. Chem. Soc.</i> 2015 , 137, 6983.
Double-gyroid MoS ₂	0.022	6.74	200	43-47	<i>Nat. Mater.</i> 2012 , 11, 963.
Edge-terminated MoS ₂	0.28	10	149	49	<i>Nat. Commun.</i> 2015 , 6, 7493.
MoS ₂ @N-doped carbon	1.0	10	165	55	<i>Angew. Chem. Int. Ed.</i> 2015 , 54, 7395.
Hierarchical MoS ₂	1.0	10	167	70	<i>Adv. Mater.</i> 2015 , DOI: 10.1002/adma.201502765
NiMoN _x /C	0.25	2	170	36	<i>Angew. Chem. Int. Ed.</i> 2012 , 51, 6131.
MoP NPs	0.36	10	125	54	<i>Adv. Mater.</i> 2014 , 26, 5702.
WC-CNTs	/	10	145	72	<i>ACS Nano</i> 2015 , 9, 5125.
P-WN/rGO	0.337	10	85	54	<i>Angew. Chem. Int. Ed.</i>

					2015, 54, 6325.
Ni ₂ P hollow particles	1	10	116	46	<i>J. Am. Chem. Soc.</i> 2013 , 135, 9267.
CoP/CNT	0.285	10	122	54	<i>Angew. Chem. Int. Ed.</i> 2014 , 126, 6828.
Cu ₃ P NWs/CF	15.2	10	143	67	<i>J. Am. Chem. Soc.</i> 2014 , 136, 7587.
Co/N-rich CNTs	0.28	10	260	69	<i>Angew. Chem. Int. Ed.</i> 2014 , 53, 4372.

Table S5. Comparison of HER performance in basic media for nanoMoC@GS with other electrocatalysts.

Catalyst	Loading (mg·cm ⁻²)	<i>j</i> (mA·cm ⁻²)	<i>η</i> (mV)	Tafel slope (m·dec ⁻¹)	Ref.
nanoMoC@GS	0.76	$\frac{1}{10}$	$\frac{43}{77}$	50	This work
MoC _x octahedrons	0.8	$\frac{1}{10}$	$\frac{92}{151}$	59	<i>Nat. Commun.</i> 2015, 6, 6512.
Mo ₂ C microparticles	0.8-2.3	20	210-240	54-59	<i>Angew. Chem. Int. Ed.</i> 2012 , 51, 12703.
MoC-Mo ₂ C HNWs	0.14 (optimal)	10	120	42	<i>Chem. Sci.</i> , 2016 , DOI: 10.1039/c6sc00077k.
Ni-Mo ₂ C nanorods	0.43	10	ca. 140	49	<i>Appl. Catal., B</i> , 2014 , 154, 232.
Mo ₂ C NTs	0.75	10	112	55	<i>Angew. Chem. Int. Ed.</i> 2015 , 54, 15395.
Mo ₂ C@NC	0.28	10	60	/	<i>Angew. Chem. Int. Ed.</i> 2015 , 54, 10752.
MCNs@carbon	0.25	10	78	41	<i>Angew. Chem. Int. Ed.</i> 2015 , 54, 14723.
WC-CNTs	/	10	165	72	<i>ACS Nano</i> 2015 , 9, 5125.
MoS ₂ nanosheet arrays	/	10	190	100	<i>Electrochim. Acta</i> 2015 , 168, 256.
MoP	0.86	10	130	48	<i>Energy Environ. Sci.</i> 2014 , 7, 2624.
Ni-Mo nanopowder	1	10	~80	/	<i>ACS Catal.</i> 2013 , 3, 166.
Co@Co- oxo/hydroxo phosphate	/	2	385	140	<i>Nat. Mater.</i> 2012 , 11, 802.
CoP NW arrays	0.92	$\frac{1}{10}$	$\frac{115}{209}$	129	<i>J. Am. Chem. Soc.</i> 2014 , 136, 7587.
NiS ₂ nanosheets	4.1	10	150	69	<i>Electrochimica Acta</i> 2015 , 153, 508.
Ni ₃ S ₂ /nickel foam	1.6	10	223	/	<i>J. Am. Chem. Soc.</i> 2015 , 137, 14023.
NiP ₂ nanosheet	4.3	10	102	64	<i>Nanoscale.</i> 2014 , 6, 13440.
WP NW arrays	2.0	10	150	102	<i>ACS Appl. Mater. Inter.</i> 2014 , 6, 21874.

Reference

- [S1] H. B. Wu, B. Y. Xia, L. Yu, X. Y. Yu and X. W. D. Lou, *Nat. commun.*, 2015, **6**, 6512.